TI medium – absorbing boundary conditions

P.F. Daley

ABSTRACT

When using pseudo – spectral methods to reduce to the spatial dimensionality of the 2.5D coupled $qP-qS_V$ wave propagation problem in a transversely isotropic (TI) medium to that in one spatial dimension and time, the introduction of an absorbing boundary, at least at the model bottom is useful in the removal of spurious arrivals. The top model boundary is usually wanted in the numerical calculations and reflections from the model sides may be removed by a judicious choice of model parameters, which does not significantly increase the run time. In this report, a method similar to that presented in Clayton and Engquist (1977, 1980) and is derived for the coupled $qP-qS_V$ wave propagation problem in a transversely isotropic medium. Finite Hankel transforms are used to remove the radial coordinate (r) in what is assumed to be a radially symmetric medium. The problem that remains is a coupled problem in depth (z), where the anisotropic parameters may arbitrarily vary, in depth and time (t).

INTRODUCTION

This method is most often referred to as the pseudo-spectral method, but due to the extensive work done in this area by B.G. Mikhailenko and A.S. Alekseev it is sometimes referred to, in seismic applications, as the Alekseev-Mikhailenko Method (AMM), (Alekseev and Mikhailenko, 1980). It falls within the genetic class of pseudo-spectral methods, but is possibly more formal and rigorous in its development. However, much of their work is relatively physically inaccessible and a considerable number of the more significant contributions are in Russian. Other works of interest in this area are Gazdag (1973), Gazdag (1981) and Kosloff and Baysal (1982).

One numerical advantage of applying finite integral transforms is that the resultant FD problem is in one spatial variable and time and there are no cross derivative terms. These are differentials of the form $\partial/\partial x_i\left[c\left(x_1,x_2,x_3\right)\partial u_k/\partial x_j\right]\quad i,j,k=1,2,3:\quad i\neq j$. Several approaches for dealing with these in a finite difference context may be found in Zahradník et al. (1993).

Apart from a number of other numerical considerations, the removal of spurious reflections from the pseudo model bottom is required. This is done here using the method described in Clayton and Engquist (1977), but modified for the transversely isotropic case. Initially, this may appear as a simple transition. However, it is slightly more complicated than is first apparent.

THEORETICAL OVERVIEW

Consider the problem of coupled $qP-qS_V$ wave propagation in a radially symmetric (no lateral inhomogeneities), vertically inhomogeneous transversely isotropic half space. The

equations of motion are defined by the elastodynamic (Navier) equations (Martynov and Mikhailenko, 1984 Mikhailenko and Korneev, 1984, or Mikhailenko, 1985, as examples)

$$\rho\frac{\partial^2 U}{\partial t^2}=c_{11}\left[\frac{\partial^2 U}{\partial r^2}+\frac{1}{r}\frac{\partial U}{\partial r}-\frac{U}{r^2}\right]+c_{13}\frac{\partial^2 V}{\partial r\partial z}+\frac{\partial}{\partial z}\left[c_{55}\left(\frac{\partial U}{\partial z}+\frac{\partial V}{\partial r}\right)\right]+\rho F_r \tag{1}$$

$$\rho\frac{\partial^2 V}{\partial t^2}=c_{55}\left[\frac{\partial}{\partial r}\left(\frac{\partial U}{\partial z}+\frac{\partial V}{\partial r}\right)+\frac{1}{r}\left(\frac{\partial U}{\partial z}+\frac{\partial V}{\partial r}\right)\right]+\frac{\partial}{\partial z}\left[c_{13}\left(\frac{\partial U}{\partial r}+\frac{U}{r}\right)+c_{33}\frac{\partial V}{\partial z}\right]+\rho F_z \tag{2}$$

where the particle displacement vector $\mathbf{u}$ is of the form

$$\mathbf{u}\equiv\mathbf{u}(r,z,t)=\left(U(r,z,t),V(r,z,t)\right). \tag{3}$$

Here $U(r,z,t)$ and $V(r,z,t)$ are the radial (horizontal) and vertical components of vector particle displacement, the azimuthal component of displacement being zero for the coupled $qP-qS_V$ problem. The coordinates r and z are the radial and vertical coordinates in a cylindrical coordinate system, respectively, t is time In Voigt notation, the c_{ij} are the stiffness parameters of the medium and ρ is the density, all of which may be dependent on the vertical (z) coordinate. The density normalized anisotropic parameters, $a_{ij}=c_{ij}/\rho$, having dimensions of velocity squared, may also be used at some points within this report.

The problem is solved subject to the initial conditions

$$\mathbf{u}\big|_{t=0}=\left.\frac{\partial\mathbf{u}}{\partial t}\right|_{t=0}=0 \tag{4}$$

and the free surface boundary conditions that are required to be satisfied are

$$\sigma_{zz}\big|_{z=0}=0, \qquad \text{and} \qquad \sigma_{rz}\big|_{z=0}=0. \tag{5}$$

That is, the normal stress and shear stress are zero at the free surface. In terms of $U(r,z,t)$, $V(r,z,t)$ and the anisotropic stiffness coefficients, c_{ij}, the expressions for the normal and shear stresses at the free surface are given by

$$\sigma_{zz}\big|_{z=0}=\left[c_{13}\left(\frac{1}{r}\frac{\partial(rU)}{\partial r}\right)+c_{33}\frac{\partial V}{\partial z}\right]=0 \tag{6}$$

$$\sigma_{rz}\big|_{z=0}=c_{55}\left(\frac{\partial U}{\partial z}+\frac{\partial V}{\partial r}\right)=0 \tag{7}$$

Introducing the finite Hankel integral transforms and the vector designation $\mathbf{G}\left(\tilde{k}_i,k_i,z,t\right)=\left(S\left(\tilde{k}_i,z,t\right),R\left(k_i,z,t\right)\right)$ has

$$S\left(\tilde{k}_i, z, t\right) = \int_0^a U\left(r, z, t\right) J_1\left(k_i r\right) r\, dr \tag{8}$$

$$R\left(k_i, z, t\right) = \int_0^a V\left(r, z, t\right) J_0\left(\tilde{k}_i r\right) r\, dr \tag{9}$$

where the k_i and $\tilde{k}_i$ are the roots of the transcendental equations

$$J_0\left(\tilde{k}_i r\right) = 0 \tag{10}$$

and

$$J_1\left(k_i r\right) = 0\,, \tag{11}$$

respectively. Using the two formulations of the Hankel transforms discussed in Appendix A, it may be shown that both of the inverse series summations may be accomplished using only the roots of one of the Bessel function transcendental equation, $J_1\left(k_i r\right) = 0$, so that the inverse transforms are defined by

$$U\left(r, z, t\right) = \frac{2}{a^2} \sum_{i=1}^{\infty} \frac{S\left(k_i, z, t\right) J_1\left(k_i r\right)}{\left[J_0\left(k_i a\right)\right]^2} \tag{12}$$

$$V\left(r, z, t\right) = \frac{2}{a^2} \sum_{i=1}^{\infty} \frac{R\left(k_i, z, t\right) J_0\left(k_i r\right)}{\left[J_0\left(k_i a\right)\right]^2} \tag{13}$$

Thus both inverse series summations may be taken over the roots of one rather than two transcendental equations and as a consequence, $\mathbf{G}\left(k_i, z, t\right) = \left(S\left(k_i, z, t\right), R\left(k_i, z, t\right)\right)$. The matter of what, numerically, constitutes an infinite number of terms in the inverse series summations is addressed in Daley (2011). It is shown there that an earlier assumption that the source wavelet be band limited is significant in this determination. As the only spatial direction in which a finite difference is used is the *z* direction the most economical manner to introduce a damping conditions at the lower *z* boundary, i.e., $\gamma_1\left(z\right)\partial R/\partial t$ and $\gamma_2\left(z\right)\partial S/\partial t$. A safe estimate for the length of this damping region is of the order of 1 wavelength *(WL)* but $2WL$ are commonly used (B.G. Mikhailenko, 1980).

Applying the appropriate Hankel transforms to equations (1) and (2) results in

$$\rho\frac{\partial^2 S}{\partial t^2}=\frac{\partial}{\partial z}\left(c_{55}\frac{\partial S}{\partial z}-k_i c_{55}R\right)-k_i c_{13}\frac{\partial R}{\partial z}-k_i^2 c_{11}S+\rho\hat{F}_r \tag{14}$$

$$\rho\frac{\partial^2 R}{\partial t^2}=\frac{\partial}{\partial z}\left(c_{33}\frac{\partial R}{\partial z}+k_i c_{13}S\right)+k_i c_{55}\frac{\partial S}{\partial z}-k_i^2 c_{55}R+\rho\hat{F}_r \tag{15}$$

while the transforms of the shear and normal stresses at the free surface, which is assumed to be planar, have the form

$$\left[c_{55}\left(\frac{\partial S}{\partial z}-k_i R\right)\right]\Big|_{z=0}=0 \tag{16}$$

$$\left(c_{33}\frac{\partial R}{\partial z}+k_i c_{13}S\right)\Big|_{z=0}=0\,. \tag{17}$$

The transformed initial conditions at $t=0$ are

$$S\left(z,k_i,t\right)\Big|_{t=0}=0;\quad R\left(z,k_i,t\right)\Big|_{t=0}=0;\quad \frac{\partial S}{\partial t}\Big|_{t=0}=\frac{\partial S}{\partial t}\Big|_{t=0}=0. \tag{18}$$

where k_i are the roots of the transcendental equation $J_1\left(k_i a\right)=0$ which requires additional boundary conditions at $r=a$ (pseudo boundary such that)

$$U\big|_{r=a}=\frac{\partial V}{\partial r}\Big|_{r=a}=0 \tag{19}$$

The pseudo boundary is placed at some distance $r=a$ so that no spurious reflections from this boundary are present in the synthetic traces. The unwanted reflections may be removed using variation of the methods described in works such as Clayton and Engquist (1977), Cerjan et al. (1985) or Reynolds (1978). Care is required in choosing this distance, as the number of terms in the inverse series summation depends on it in a linear fashion. More on this may be found in Daley (2011).

If it is assumed that the anisotropic parameters (stiffness coefficients) are spatially independent the Hankel transformed equations take on the simplified forms given below. For convenience, it is assumed that the first two grid points in $z\left(z_0 \text{ and } z_1\right)$, at the free surface are of this form so that equations (14) and (15) may be written there as

$$\frac{\partial^2 S}{\partial t^2} = a_{55}\frac{\partial^2 S}{\partial z^2} - k_i\left(a_{13}+a_{55}\right)\frac{\partial R}{\partial z} - k_i^2 a_{11} S \tag{20}$$

$$\frac{\partial^2 R}{\partial t^2} = a_{33}\frac{\partial^2 R}{\partial z^2} + k_i\left(a_{13}+a_{55}\right)\frac{\partial S}{\partial z} - k_i^2 a_{55} R \tag{21}$$

and the Hankel transformed shear and normal stresses required at the free surface as boundary conditions have been given in equations (16) and (17).

An explicit finite difference scheme will be introduced into the transformed equations in depth and time $\left(z \text{ and } t\right)$. Equal grid spacing of h in the z direction and δ in time so that an arbitrary depth and time point are specified by $z_k = nh$ and $t_m = m\delta$. The order of accuracy of the finite difference process is 2nd order, $O\left(h^2, \delta^2\right)$.

An explosive point $P-$wave source is most commonly used in producing synthetic seismograms using this method. The transformed radial and vertical components of the source term are given as

$$\hat{F}_r = \frac{1}{2\pi}\delta\left(z-d\right) f\left(t\right) \tag{22}$$

$$F_z = \frac{1}{2\pi}\frac{d}{dz}\left[\delta\left(z-d\right)\right] f\left(t\right) \tag{23}$$

where $\delta\left(\zeta\right)$ is the Dirac delta function and $f\left(t\right)$ is the time dependence of the source wavelet, which is assumed to be band limited.

ABSORBING BOUNDARY AT MODEL BOTTOM

If it is assumed that the last 3 grid points in depth are homogeneous (independent of *z*) so that the Hankel transformed equations of motion have the form

$$a_{55}\frac{\partial^2 S}{\partial z^2} - k_i\left(a_{13}+a_{55}\right)\frac{\partial R}{\partial z} - k_i^2 a_{11} S - \frac{\partial^2 S}{\partial t^2} = 0 \tag{24}$$

$$a_{33}\frac{\partial^2 R}{\partial z^2} + k_i\left(a_{13}+a_{55}\right)\frac{\partial S}{\partial z} - k_i^2 a_{55} R - \frac{\partial^2 R}{\partial t^2} = 0 \tag{25}$$

and a plane wave solution is assumed as

$$R \propto exp\left[-i\omega t + ik_z z\right] \qquad \text{and} \qquad S \propto exp\left[-i\omega t + ik_z z\right] \tag{26}$$

Pseudo-differential operators are defined as

$$(-i\omega) \rightarrow \frac{\partial}{\partial t} \qquad \text{and} \qquad (ik_z) \rightarrow \frac{\partial}{\partial z} \tag{27}$$

Applying the plane wave solution to equations (24) and (25) the results are

$$a_{55}(ik_z)^2 S - k_i (a_{13} + a_{55})(ik_z) R - k_i^2 a_{11} S - (-i\omega)^2 S = 0 \tag{28}$$

$$a_{33}(ik_z)^2 R + k_i (a_{13} + a_{55})(ik_z) S - k_i^2 a_{55} R - (-i\omega)^2 R = 0 \tag{29}$$

Putting (28) and (29) in matrix form has, with **I** being the (2×2) identity matrix,

$$\begin{aligned}(ik_z)^2 \begin{bmatrix} a_{55} & 0 \\ 0 & a_{33} \end{bmatrix} \begin{bmatrix} S \\ R \end{bmatrix} + k_i (ik_z) \begin{bmatrix} 0 & -(a_{13}+a_{55}) \\ (a_{13}+a_{55}) & 0 \end{bmatrix} \begin{bmatrix} S \\ R \end{bmatrix} - \\ k_i^2 \begin{bmatrix} a_{11} & 0 \\ 0 & a_{55} \end{bmatrix} \begin{bmatrix} S \\ R \end{bmatrix} - (-i\omega)^2 \mathbf{I} \begin{bmatrix} S \\ R \end{bmatrix} = 0\end{aligned} \tag{30}$$

Further rearrangement of the above equation is of the form

$$\begin{aligned}\frac{(ik_z)^2}{(-i\omega)^2} \begin{bmatrix} a_{55} & 0 \\ 0 & a_{33} \end{bmatrix} \begin{bmatrix} S \\ R \end{bmatrix} + \frac{k_i (ik_z)}{(-i\omega)^2} \begin{bmatrix} 0 & -(a_{13}+a_{55}) \\ (a_{13}+a_{55}) & 0 \end{bmatrix} \begin{bmatrix} S \\ R \end{bmatrix} - \\ \frac{k_i^2}{(-i\omega)^2} \begin{bmatrix} a_{11} & 0 \\ 0 & a_{55} \end{bmatrix} \begin{bmatrix} S \\ R \end{bmatrix} - \mathbf{I} \begin{bmatrix} S \\ R \end{bmatrix} = 0\end{aligned} \tag{31}$$

An initial approximation to the above is obtained by truncating (31) to read

$$\begin{aligned}\frac{(ik_z)^2}{(-i\omega)^2} \begin{bmatrix} a_{55} & 0 \\ 0 & a_{33} \end{bmatrix} \begin{bmatrix} S \\ R \end{bmatrix} - \mathbf{I} \begin{bmatrix} S \\ R \end{bmatrix} = 0 \\ \frac{(ik_z)^2}{(-i\omega)^2} \begin{bmatrix} a_{55} & 0 \\ 0 & a_{33} \end{bmatrix} - \begin{bmatrix} 1 & 0 \\ 0 & 1 \end{bmatrix} = 0\end{aligned} \tag{32}$$

and yields

$$\begin{aligned} a_{55} \frac{(ik_z)^2}{(-i\omega)^2} - 1 = 0 \quad &\rightarrow \quad \frac{(ik_z)}{(-i\omega)} = \frac{1}{\sqrt{a_{55}}} \\ a_{33} \frac{(ik_z)^2}{(-i\omega)^2} - 1 = 0 \quad &\rightarrow \quad \frac{(ik_z)}{(-i\omega)} = \frac{1}{\sqrt{a_{33}}} \end{aligned} \tag{33}$$

This preliminary approximation is not generally used in practice, but rather to enable the solution of (31). In matrix form (31) now appears as

$$\frac{(ik_z)}{(-i\omega)}\begin{bmatrix}1 & 0\\ 0 & 1\end{bmatrix}-\begin{bmatrix}1/\sqrt{a_{55}} & 0\\ 0 & 1/\sqrt{a_{33}}\end{bmatrix}=0 \tag{34}$$

Defining

$$\mathbf{A}=\begin{bmatrix}a_{55} & 0\\ 0 & a_{33}\end{bmatrix} \quad \text{has} \quad \mathbf{A}^{-1}=\begin{bmatrix}1/a_{55} & 0\\ 0 & 1/a_{33}\end{bmatrix} \tag{35}$$

Return to (30) with (34) and (35) results in

$$\frac{(ik_z)^2}{(-i\omega)^2}\begin{bmatrix}a_{55} & 0\\ 0 & a_{33}\end{bmatrix}=\left[\mathbf{I}-\frac{k_i(ik_z)}{(-i\omega)^2}\begin{bmatrix}0 & -(a_{13}+a_{55})\\ (a_{13}+a_{55}) & 0\end{bmatrix}+\frac{k_i^2}{(-i\omega)^2}\begin{bmatrix}a_{11} & 0\\ 0 & a_{55}\end{bmatrix}\right] \tag{36}$$

and then as

$$\frac{(ik_z)^2}{(-i\omega)^2}\mathbf{I}=\left[\mathbf{I}-\frac{k_i(ik_z)}{(-i\omega)^2}\begin{bmatrix}0 & -(a_{13}+a_{55})\\ (a_{13}+a_{55}) & 0\end{bmatrix}+\frac{k_i^2}{(-i\omega)^2}\begin{bmatrix}a_{11} & 0\\ 0 & a_{55}\end{bmatrix}\right]\mathbf{A}^{-1} \tag{37}$$

Approximating the above by conventional means has

$$\frac{(ik_z)}{(-i\omega)}\mathbf{I}\approx\left[\mathbf{I}-\frac{k_i(ik_z)}{(-i\omega)^2}\begin{bmatrix}0 & -(a_{13}+a_{55})\\ (a_{13}+a_{55}) & 0\end{bmatrix}+\frac{k_i^2}{(-i\omega)^2}\begin{bmatrix}a_{11} & 0\\ 0 & a_{55}\end{bmatrix}\right]^{1/2}\left(\mathbf{A}^{-1}\right)^{1/2} \tag{38}$$

where

$$\left(\mathbf{A}^{-1}\right)^{1/2}=\begin{bmatrix}1/\sqrt{a_{55}} & 0\\ 0 & 1/\sqrt{a_{33}}\end{bmatrix} \tag{39}$$

It is convenient at this point to define three (2×2) matrices $\mathbf{X}_j$ $(j=1,2,3)$ as

$$\mathbf{X}_1 = \mathbf{I}\left(\mathbf{A}^{-1}\right)^{1/2} = \begin{bmatrix} 1/\sqrt{a_{55}} & 0 \\ 0 & 1/\sqrt{a_{33}} \end{bmatrix} \tag{40}$$

$$\mathbf{X}_2 = \begin{bmatrix} 0 & -\left(a_{13}+a_{55}\right) \\ \left(a_{13}+a_{55}\right) & 0 \end{bmatrix}\left(\mathbf{A}^{-1}\right)^{1/2} = \begin{bmatrix} 0 & -\left(a_{13}+a_{55}\right)/\sqrt{a_{33}} \\ \left(a_{13}+a_{55}\right)/\sqrt{a_{55}} & 0 \end{bmatrix} \tag{41}$$

$$\mathbf{X}_3 = \begin{bmatrix} a_{11} & 0 \\ 0 & a_{55} \end{bmatrix}\left(\mathbf{A}^{-1}\right)^{1/2} = \begin{bmatrix} a_{11} & 0 \\ 0 & a_{55} \end{bmatrix}\begin{bmatrix} 1/\sqrt{a_{55}} & 0 \\ 0 & 1/\sqrt{a_{33}} \end{bmatrix} = \begin{bmatrix} a_{11}/\sqrt{a_{55}} & 0 \\ 0 & a_{55}/\sqrt{a_{33}} \end{bmatrix} \tag{42}$$

so that (38) may be written as

$$\left(ik_z\right)\left(-i\omega\right)\mathbf{I} \approx \left[\mathbf{X}_1\left(-i\omega\right)^2 - \frac{k_i\left(ik_z\right)}{2}\bar{\mathbf{X}}_2 + \frac{k_i^2}{2}\mathbf{X}_3\right] \tag{43}$$

This expression leads to the two equations

$$\left(ik_z\right)\left(-i\omega\right)S - 1/\sqrt{a_{55}}\left(-i\omega\right)^2 S - \frac{k_i\left(ik_z\right)}{2}\left(a_{13}+a_{55}\right)/\sqrt{a_{33}}\,R - \frac{k_i^2}{2}a_{11}/\sqrt{a_{55}}\,S = 0 \tag{44}$$

and

$$\left(ik_z\right)\left(-i\omega\right)R - 1/\sqrt{a_{33}}\left(-i\omega\right)^2 R + \frac{k_i\left(ik_z\right)}{2}\left(a_{13}+a_{55}\right)/\sqrt{a_{55}}\,S - \frac{k_i^2}{2}a_{55}/\sqrt{a_{33}}\,R = 0 \tag{45}$$

When the pseudo-differential operators are introduced the follow equations are the 15° approximations to the absorbing equations at the model bottom.

$$\frac{\partial^2 S}{\partial z \partial t} - \frac{1}{\sqrt{a_{55}}}\frac{\partial^2 S}{\partial t^2} - \frac{k_i\left(a_{13}+a_{55}\right)}{2\sqrt{a_{33}}}\frac{\partial R}{\partial z} - \frac{k_i^2 a_{11}}{2\sqrt{a_{55}}}S = 0 \tag{46}$$

$$\frac{\partial^2 R}{\partial z \partial t} - \frac{1}{\sqrt{a_{33}}}\frac{\partial^2 R}{\partial t^2} + \frac{k_i\left(a_{13}+a_{55}\right)}{2\sqrt{a_{55}}}\frac{\partial S}{\partial z} - \frac{k_i^2 a_{55}}{2\sqrt{a_{33}}}R = 0 \tag{47}$$

With $\mathbf{G} = \left(S, R\right)$ and using the finite difference template introduced in Clayton and Engquist (1977) the following definition may be employed

$$D_-^z D_0^t \mathbf{G}_K^n - \left(\frac{1}{2}\right)\mathbf{X}_1 D_+^t D_-^t \left(\mathbf{G}_K^n + \mathbf{G}_{K-1}^n\right) - \left(\frac{1}{4}\right)\mathbf{X}_2 D_+^z \left(\mathbf{G}_K^{n-1} + \mathbf{G}_{K-1}^n\right) - \left(\frac{1}{4}\right)\mathbf{X}_3 \left(\mathbf{G}_K^{n-1} + \mathbf{G}_{K-1}^n\right) = 0 \tag{48}$$

where the $\mathbf{X}_j \ (j = 1, 2, 3)$ have been redefined as

$$\mathbf{X}_1 = \mathbf{X}_1 , \qquad \mathbf{X}_2 = k_j \mathbf{X}_2 , \qquad \mathbf{X}_3 = k_j^2 \mathbf{X}_3 \tag{49}$$

The operators D_+^q, D_-^q and D_0^q are the forward, backward and center difference finite difference analogues with respect to the variable q and are defined as

$$\text{Forward}: \quad D_+^z G_k^n \approx \left(G_{k+1}^n - G_k^n\right)\Big/\Delta z \tag{50}$$

$$\text{Backward}: \quad D_-^z G_k^n \approx \left(G_k^n - G_{k-1}^n\right)\Big/\Delta z \tag{51}$$

$$\text{Center}: \quad D_0^t G_k^n \approx \left(G_k^{n+1} - G_k^{n-1}\right)\Big/\left(2\Delta t\right)$$

$$\text{actually} \quad D_0^t G_k^n \approx \left(G_k^{n+1/2} - G_k^{n-1/2}\right)\Big/\Delta t \tag{52}$$

Employing these relations the following intermediate results are obtained:

$$D_-^z D_0^t S_K^n \approx D_-^z \left(\frac{S_K^{n+1} - S_K^{n-1}}{2\Delta t}\right) \approx \left(\frac{S_K^{n+1} - S_{K-1}^{n+1}}{2h\Delta t}\right) - \left(\frac{S_K^{n-1} - S_{K-1}^{n-1}}{2h\Delta t}\right) = \left(\frac{S_K^{n+1} - S_{K-1}^{n+1} - S_K^{n-1} + S_{K-1}^{n-1}}{2h\Delta t}\right) \tag{53}$$

$$D_-^z D_0^t R_K^n \approx D_-^z \left(\frac{R_K^{n+1} - R_K^{n-1}}{2\Delta t}\right) \approx \left(\frac{R_K^{n+1} - R_{K-1}^{n+1}}{2h\Delta t}\right) - \left(\frac{R_K^{n-1} - R_{K-1}^{n-1}}{2h\Delta t}\right) = \left(\frac{R_K^{n+1} - R_{K-1}^{n+1} - R_K^{n-1} + R_{K-1}^{n-1}}{2h\Delta t}\right) \tag{54}$$

$$D_+^t D_-^t \left(S_K^n + S_{K-1}^n\right) \approx \left(\frac{S_K^{n+1} - 2S_K^n + S_K^{n-1}}{\left(\Delta t\right)^2}\right) + \left(\frac{S_{K-1}^{n+1} - 2S_{K-1}^n + S_{K-1}^{n-1}}{\left(\Delta t\right)^2}\right) = \left(\frac{S_K^{n+1} - 2S_K^n + S_K^{n-1} + S_{K-1}^{n+1} - 2S_{K-1}^n + S_{K-1}^{n-1}}{\left(\Delta t\right)^2}\right) \tag{55}$$

$$D_+^t D_-^t \left(R_K^n + R_{K-1}^n \right) \approx \left(\frac{R_K^{n+1} - 2R_K^n + R_K^{n-1}}{\left(\Delta t\right)^2} \right) + \left(\frac{R_{K-1}^{n+1} - 2R_{K-1}^n + R_{K-1}^{n-1}}{\left(\Delta t\right)^2} \right) = \left(\frac{R_K^{n+1} - 2R_K^n + R_K^{n-1} + R_{K-1}^{n+1} - 2R_{K-1}^n + R_{K-1}^{n-1}}{\left(\Delta t\right)^2} \right) \tag{56}$$

$$D_-^z \left(S_K^n + S_{K-1}^n \right) \approx \left(\frac{S_K^{n-1} - S_{K-1}^{n-1}}{h} \right) + \left(\frac{S_{K-1}^n - S_{K-2}^n}{h} \right) \tag{57}$$

Introducing equations (53) – (57) into (48) results in the following two equations for the transformed radial and vertical components of the paraxial wave equation approximation for the absorbing boundary conditions at the model bottom for the problem considered here:

Radial:

$$S_K^{n+1} = \left[S_{K-1}^{n+1} + S_K^{n-1} - S_{K-1}^{n-1} + \frac{\mathbf{X}_1^{11}\Delta z}{\Delta t}\left(-2S_K^n + S_K^{n-1} + S_{K-1}^{n+1} - 2S_{K-1}^n + S_{K-1}^{n-1} \right) + \frac{\mathbf{X}_2^{12}\Delta t}{2}\left(R_K^{n-1} - R_{K-1}^{n-1} + R_{K-1}^n - R_{K-2}^n \right) + \frac{\mathbf{X}_3^{11}\Delta z \Delta t}{2}\left(S_K^{n-1} + S_{K-1}^n \right) \right] \Big/ \left(1 - \frac{\mathbf{X}_1^{11}\Delta z}{\Delta t} \right) \tag{58}$$

Vertical:

$$R_K^{n+1} = \left[R_{K-1}^{n+1} + R_K^{n-1} - R_{K-1}^{n-1} + \frac{\mathbf{X}_1^{22}\Delta z}{\Delta t}\left(-2R_K^n + R_K^{n-1} + R_{K-1}^{n+1} - 2R_{K-1}^n + R_{K-1}^{n-1} \right) + \frac{\mathbf{X}_2^{21}\Delta t}{2}\left(S_K^{n-1} - S_{K-1}^{n-1} + S_{K-1}^n - S_{K-2}^n \right) - \frac{\mathbf{X}_3^{22}\Delta z \Delta t}{2}\left(R_K^{n-1} + R_{K-1}^n \right) \right] \Big/ \left(1 - \frac{\mathbf{X}_1^{22}\Delta z}{\Delta t} \right) \tag{59}$$

NUMERICAL RESULTS

The model used for testing the absorbing boundary conditions at the model bottom of a plane layered transversely isotropic media is given in Table 1 and Figure (1). The recording geometry is a vertical seismic profile (VSP) with a surface source offset $250m\left(0.25km\right)$ from the well bore. The receivers are located in the well bore at depths from $150m\left(0.15km\right)$ to $1900m\left(1.9km\right)$ at $12.5m\left(0.0125km\right)$ intervals. Numerical experiments, based on the isotropic case, have indicated that the 15 degree paraxial approximations to the equations of motion to introduce damping may appear not to be the optimal manner of proceeding. Much of this is a consequence of the display options available in the CREWES toolbox. It is much too easy to introduce scaling (high clip) leading to noise having amplitude of the order of the seismic signal. To overcome this, the 15 degree approximation is used until it is determined that what may appear to be spurious arrivals due to high clip begin to be seen. At this point, the finite difference computations are terminated. To compensate for this, a input parameter has been introduced that has the effect of allowing for the required length in time of the synthetic traces may be obtained. This is shown in the two panels in Figures (2) and (4) (vertical and radial components). The full

synthetics for the vertical and radial components are shown in Figures (3) and (5) using the CREWES toolbox utility *plotseismic* . The same results (vertical and radial components) using the utility *plotimage* are shown in Figures (6) and (7). It is clear that there are no spurious arrivals appearing in the synthetic traces, even at a level of high scaling. This refinement comes at a quite minimal cost in run time.

CONCLUSIONS

Using the paper of Clayton and Engquist (1977), which treats seismic wave propagation for the coupled $P-S_V$ modes in a $2D$ elastic medium, as a template, absorbing boundary conditions are derived for the model bottom boundary in a transversely isotropic medium. A vertically inhomogeneous medium has been assumed with the radial derivatives of particle motion being transformed away using finite Hankel transforms. This produces a coupled set of equations for the vertical and radial components of displacement that are to be solved using finite difference methods in the remaining spatial coordinate depth (z) and time. This problem is at least marginally different than what appears in Clayton and Engquist (1977), but a similar solution method may be employed. What results are the so called 15 degree paraxial approximations to the equations of particle displacement. Numerical experiments have shown that what was derived provides a reasonable solution and does remove spurious reflections from the model bottom, if the synthetics are not "over scaled". A modification was introduced to account for the effects of unwanted arrivals appearing in the synthetics when various forms of scaling are introduced. This alteration is a temporary measure and other forms of damping are being considered, specifically some form of exponential damping.

REFERENCES

Alekseev, A.S. and Mikhailenko, B.G., 1980, Solution of dynamic problems of elastic wave propagation in inhomogeneous media by a combination of partial separation of variables and finite difference methods, Journal of Geophysics, 48, 161-172.

Cerjan, C., Kosloff, D., Kosloff, R. and Reshef, M., 1985, A nonreflecting boundary condition for discrete acoustic and elastic wave equations, Geophysics, 50, 705-708.

Clayton, R. and Engquist, B., 1977, Absorbing boundary conditions for acoustic and elastic wave equations, Bulletin of the Seismological Society of America, 67, 1529-1540.

Clayton, R. and Engquist, B., 1980, Absorbing boundary conditions for wave-equation migration, GEOPHYSICS, 45, 895-904.

Daley, P.F., 2011, *P*-S_V wave propagation in a radially symmetric vertically inhomogeneous TI medium: Finite difference hybrid method, CREWES Research Report, Volume 23.

Gazdag, J., 1973, Numerical convective schemes based on the accurate computation of space derivatives, Journal of Computational Physics, 13, 100-113.

Gazdag, J., 1981, Modeling of the acoustic wave equation with transform methods, Geophysics, 46, 854-859.

Kosloff, D. and Baysal, E., 1982, Forward modeling by a Fourier method, Geophysics, 47, 1402-1412.

Martynov, V.N. and Mikhailenko, B.G., 1984, Numerical modelling of propagation of elastic waves in anisotropic inhomogeneous media for the half-space and the sphere, Geophysical Journal of the Royal Astronomical Society, 76, 53-63.

Mikhailenko, B.G., 1980, Personal communication.

Mikhailenko, B.G. and Korneev, V.I., 1984,Calculation of synthetic seismograms for complex subsurface geometries by a combination of finite integral Fourier transforms and finite difference techniques, Journal of Geophysics, 54, 195-206.

Mikhailenko, B.G., 1985, Numerical experiment in seismic investigations, Journal of Geophysics, 58, 101-124.

Reynolds, A.C., 1978, Boundary conditions for the numerical solution of wave propagation problems, Geophysics, 43, 1099-1110.

Zahradnik, J., P. Moczo, and F. Hron, 1993, Testing four elastic finite difference schemes for behavior at discontinuities, Bulletin of the Seismological Society of America, 83, 107-129.

ACKNOWLEDGEMENTS

The first author wishes to thank the sponsors of CREWES and NSERC (Professor G.F. Margrave, CRDPJ 379744-08) for financial support in undertaking this work.

Thickness	**Density**	$\mathbf{A_{11}}$	$\mathbf{A_{33}}$	$\mathbf{A_{55}}$	$\mathbf{A_{13}}$
0.5	1.0	5.0	4.0	2.0	1.12
0.5	1.0	7.0	6.25	2.25	2.17
0.5	1.0	11.0	9.0	3.0	3.22
Hspace	1.0	16.0	12.96	3.75	4.74

Table 1: The parameters for the transversely isotropic plane layered medium used in testing the model bottom absorbing boundary condition are given in the table. Density is in gm/cm^3, thickness in *km* and the A_{ij} in km^2/s^2.

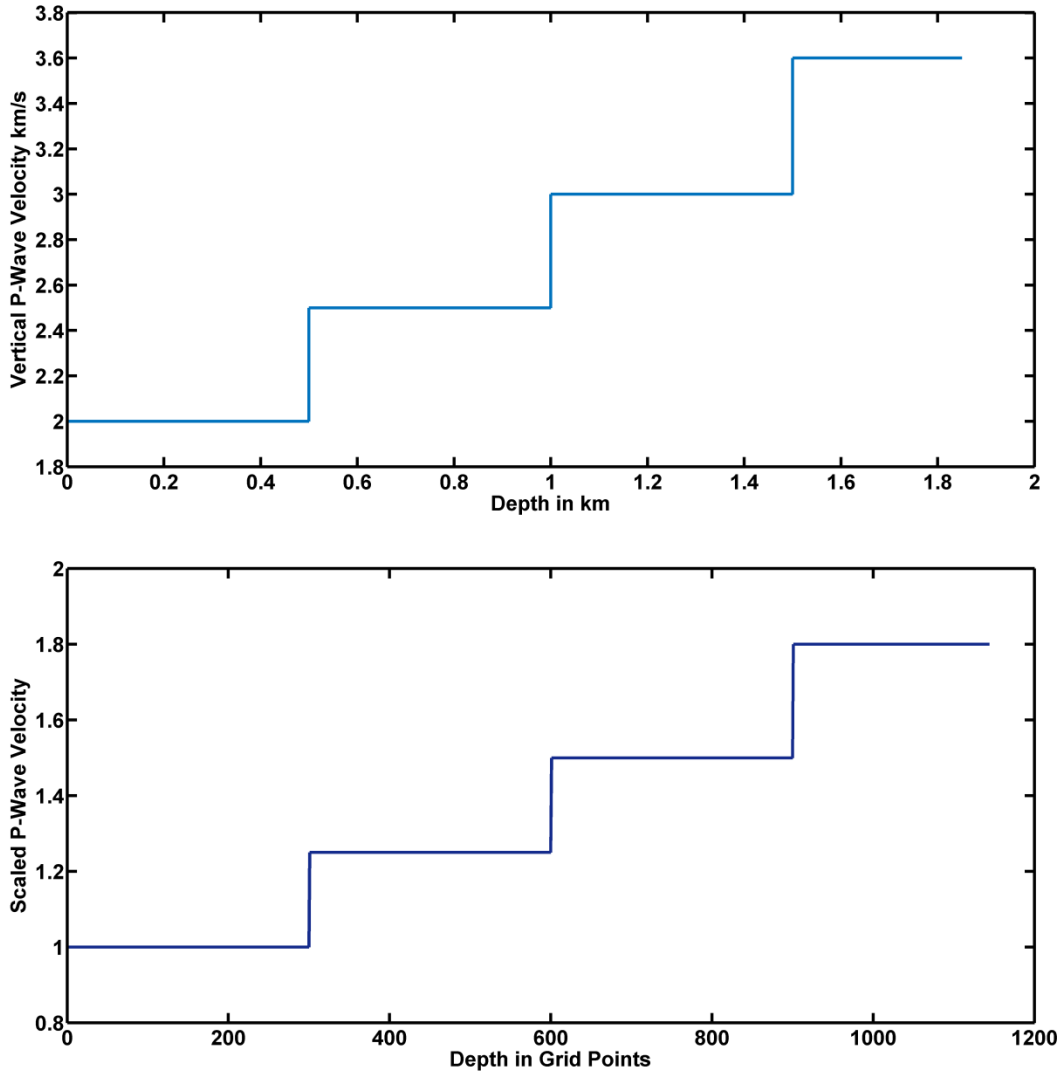

Figure 1: The vertical *P* – wave velocity in *km/s* plotted versus depth in *km* in the upper panel. In the lower panel the scaled velocity is plotted versus the number of depth grid points.

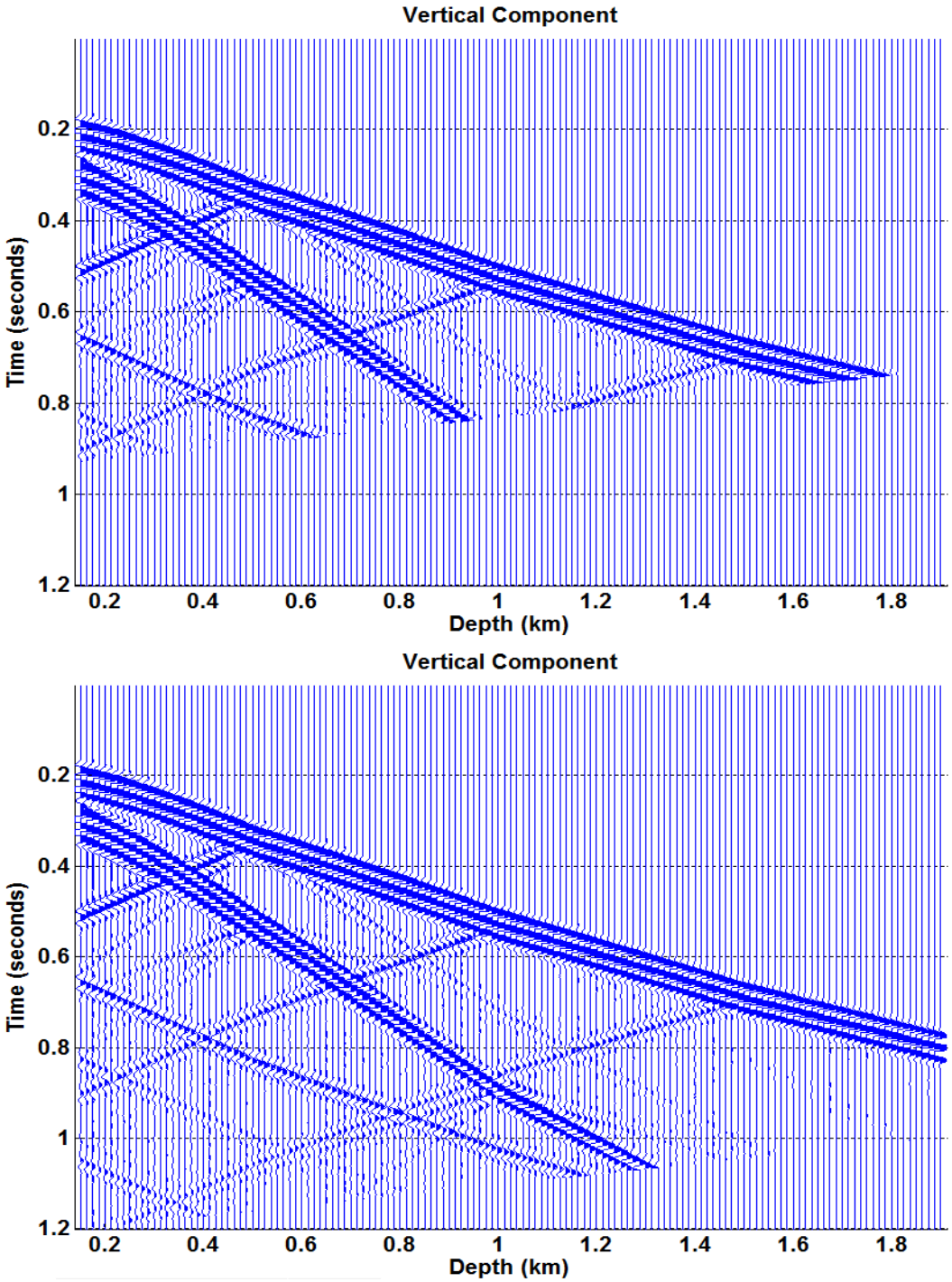

Figure 2: The two panels in this figure are examples where the computation was halted as the spurious arrivals (reflections) from the model bottom became of the order of the noise. Two examples od the vertical component are shown for a VSP with a surface source located at 250*m* (0.250*km*) from the bore hole.

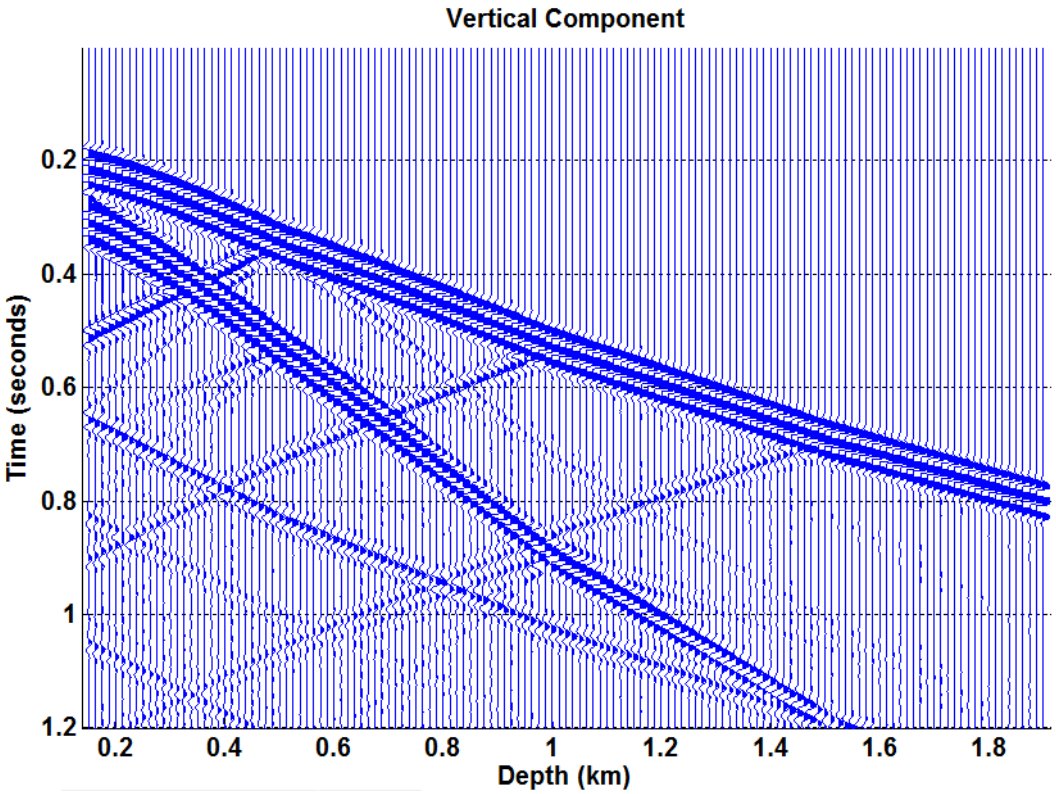

Figure 3: The vertical component of the VSP synthetic of the model described in the text. In this panel the computations continued to the proper time indicating that no spurious reflections from the model are included in the traces.

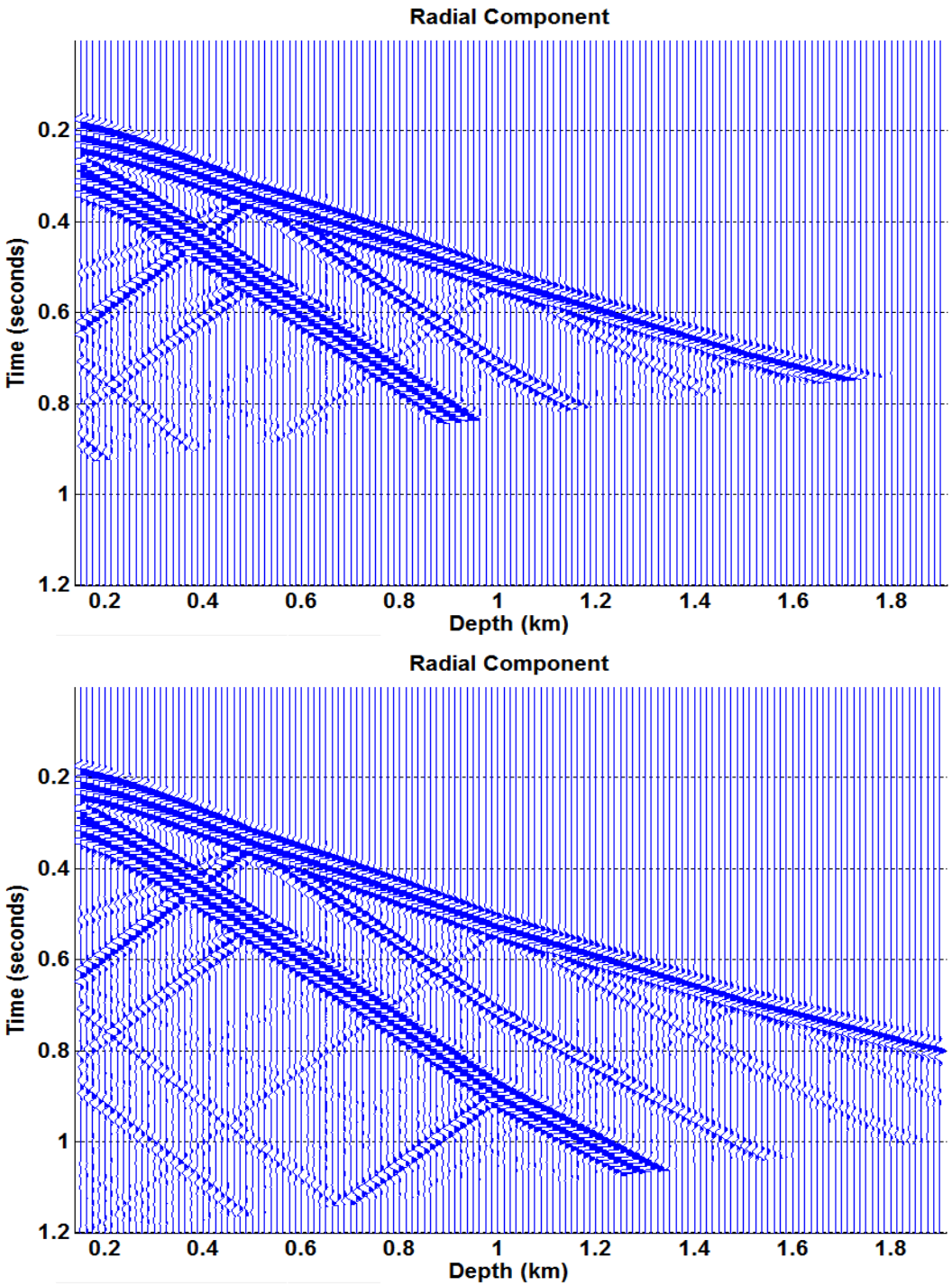

Figure 4: The two panels in this figure are examples where the computation was halted as the spurious arrivals (reflections) from the model bottom became of the order of the noise. Two examples of the radial component are shown for a VSP with a surface source located at 250*m* (0.250*km*) from the bore hole.

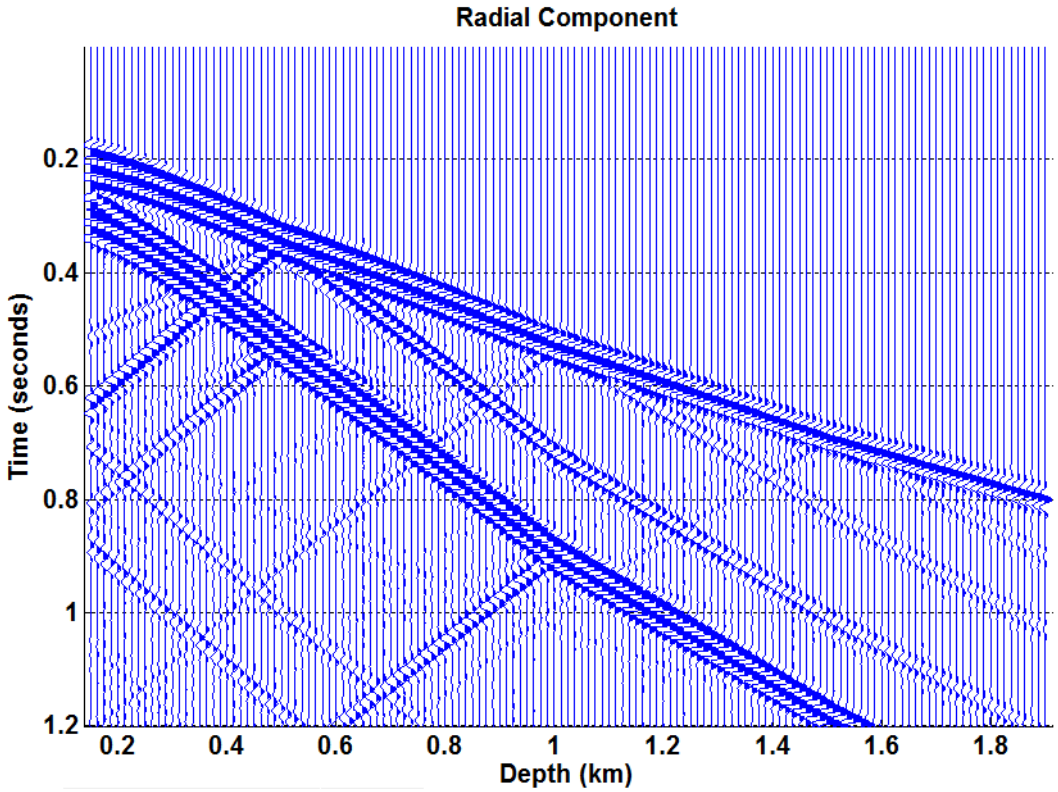

Figure 5: The radial component of the VSP synthetic of the model described in the text. In this panel the computations continued to the proper time indicating that no spurious reflections from the model are included in the traces.

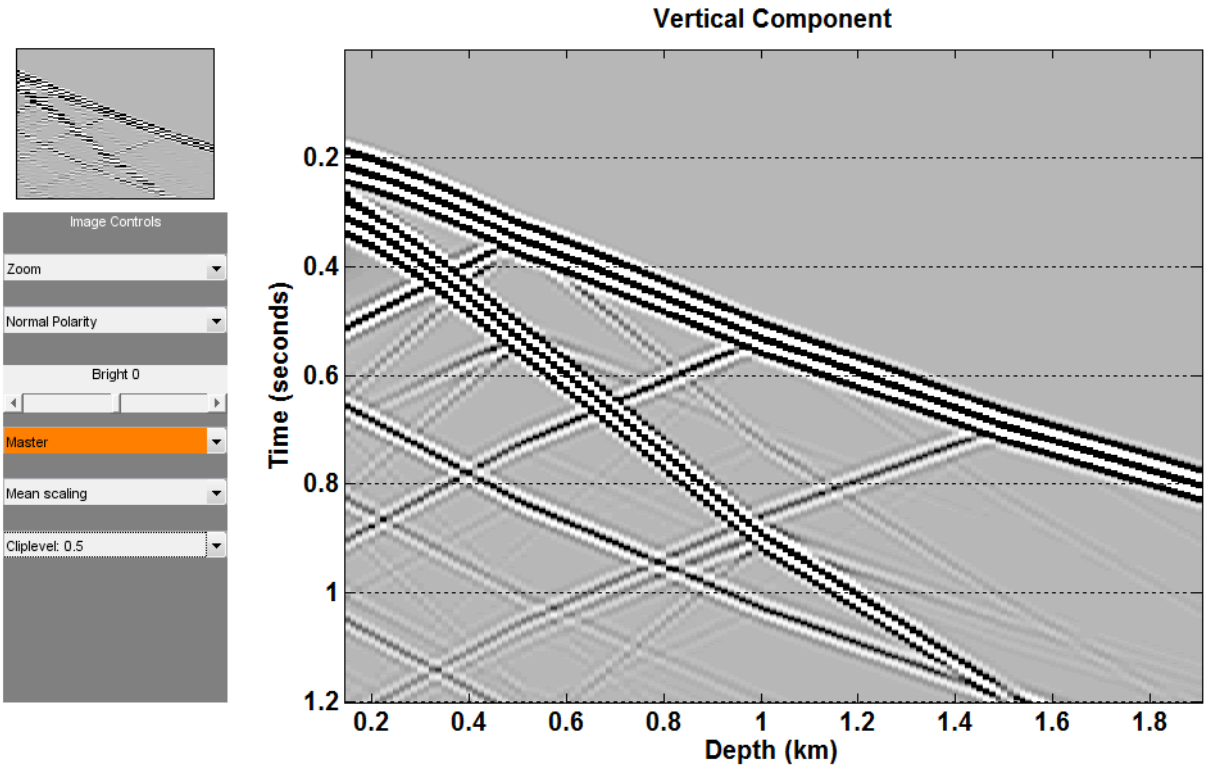

Figure 6: The vertical component of the VSP synthetic of the model described in the text. In this panel the computations continued to the proper time indicating that no spurious reflections from the model are included in the traces..Plotted with *plotimage* and is the *master* of the following figure.

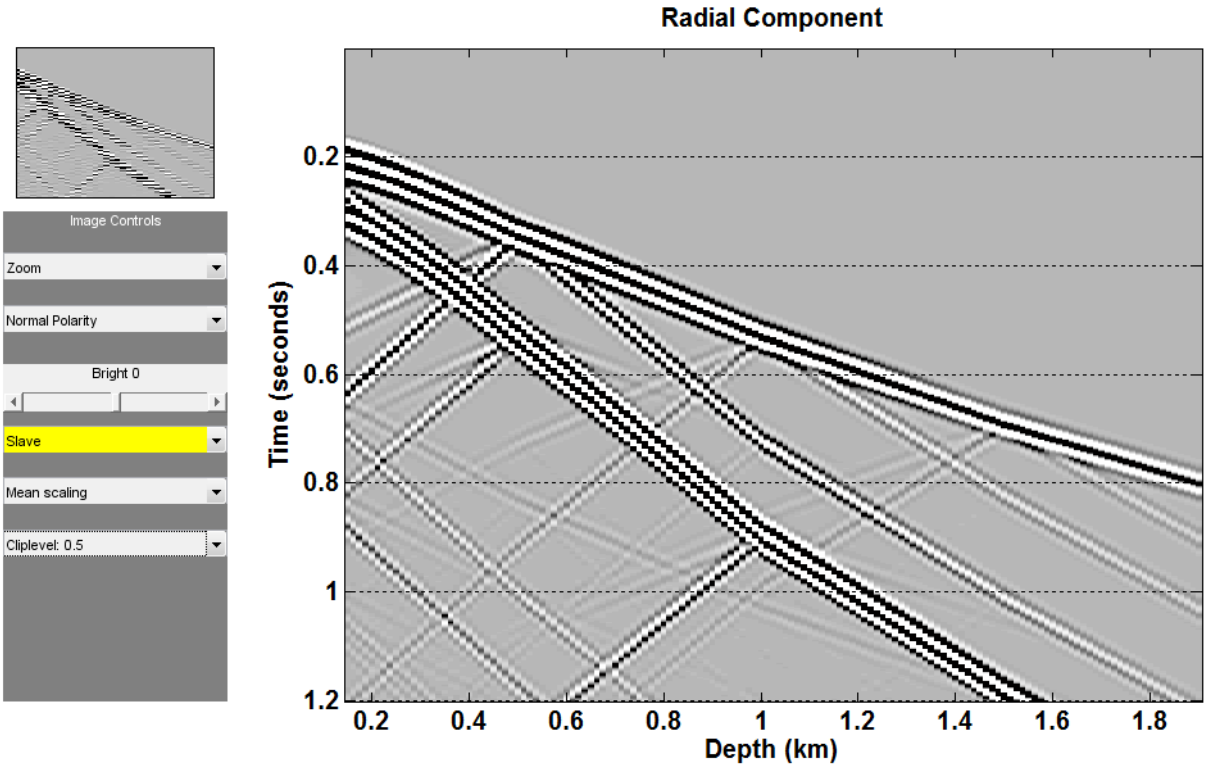

Figure 7: The radial component of the VSP synthetic of the model described in the text. In this panel the computations continued to the proper time indicating that no spurious reflections from the model are included in the traces. Plotted with *plotimage* and a *slave* of the *master* in the previous figure.